

1 of 1

Conf-940711--2
CONF-940397--1

RICH FLAMMABILITY LIMITS IN $CH_3OH/CO/DILUENT$ MIXTURES

MARY N. BUI-PHAM, ANDREW E. LUTZ, and JAMES A. MILLER

Combustion Research Facility, MS 9055

Sandia National Laboratories, Livermore, California 94551-0969

and

MICHAEL DESJARDIN, DANIEL M. O'SHAUGHNESSEY, and ROBERT J. ZONDLAK

Dow Chemical Company

Midland, Michigan 48667

Correspondence:

All correspondence should be directed to M. N. Bui-Pham at the above address, Tel: (510) 294-1464, Fax: (510) 294-2276, E-mail: mnbuiph@ca.sandia.gov

Word Count:

7 Figures + 1 Table: 1600 words

Text and Eqs.: 3621 (8 1/2 pages @ 426 words/page)

Refs.: 224

Total: 5445 words

Presentation Preference:

Oral

Publication Preference:

Proceedings

General Approach:

B. Numerical Modeling

E. Experimental Data and Interpretation

Subjects:

(1.2) Combustion Chemistry – Detailed Reaction Mechanisms

(3.1) Flames – Ignition

(3.2) Flames – Extinction

(3.4) Flames – Laminar Flames (Premixed)

(4.3) Fires – Fuels Flammability

MASTER

DISTRIBUTION OF THIS DOCUMENT IS UNLIMITED

Rich Flammability Limits in $CH_3OH/CO/diluent$ Mixtures

Mary N. Bui-Pham*, Andrew E. Lutz, and James A. Miller

Sandia National Laboratories

Livermore, CA 94551-0969

Michael Desjardin, Daniel M. O'Shaughnessey, and Robert J. Zondlak

Dow Chemical Company

Midland, MI 48607

Abstract

This research is a joint project between Sandia National Laboratories/California and the Dow Chemical Company/Midland to examine the existing flame modeling capability developed at Sandia to model experimental data for rich flammability limits. The system studied is methanol/carbon monoxide/diluent mixtures, where the diluent is either nitrogen or carbon dioxide at pressures of 1, 11, and 21 atm, respectively. The critical oxygen concentration needed to sustain a flame was experimentally determined in a spherical vessel with a central ignition source for several mixtures and pressures. Burning velocities of 1-D, planar, freely propagating premixed flames were calculated to determine the minimum oxygen concentration required for these flames to propagate. This minimum O_2 concentration was found to be consistently larger than that observed in experiments; however, the effects of pressure and diluent composition agreed well with experimental data. In order to understand better all the phenomena involved, attempts were made to model the spherical vessel experiment directly, which resulted in qualitative agreement with experimental data and steady flame predictions. In addition, the rich flammability limit was calculated for pure methanol-air flames to be

*Post-doctoral Appointee

at an equivalence ratio of ~ 2.1 , and extinction occurs at $K_{ex} = 1670 \text{ sec}^{-1}$ for the opposed-flow, strained, stoichiometric methanol-air case.

Introduction

Flammability limits are employed in the chemical industry by process engineers as guidelines to design and operate chemical facilities safely that contain combustible material. By considering these limits, the safest allowable approach to the flammable envelope for any given chemical process can be established for corporate safety and loss prevention policy. Typically, rich flammability limits where the oxidizer is restricted are difficult to estimate and must be measured. Experimental tests, such as ASTM E 918-83, are used to determine upper flammable limits for a specific composition, temperature, and pressure. However, after the process has begun operation, the chemical composition or process conditions may change, which can require additional experiments. The testing process can involve many months of work for even minor changes.

Rich flammability consideration was initiated for a new process being developed by the Dow Chemical Company, which contains methanol and carbon monoxide in an oxidizing atmosphere. This production operated in the upper-end of the flammability envelope, and since the development efforts were at an early stage, diluent gases of carbon dioxide and nitrogen were considered along with a range of process conditions. The objective of this joint project is to test the existing modeling capabilities at Sandia National Laboratories/California in predicting flammability limits for these mixtures, which will lessen the amount of experiments required to develop the process fully.

The first part of our study involves developing a chemical kinetic mechanism that can properly predict rich flame conditions. To achieve this goal, we investigated the structure and burning velocity profiles of freely propagating methanol-air premixed flames for a range of equivalence ratios from 0.6 to 2.2, comparing theoretical predictions with experimental data. We also established an extinction limit for the stoichiometric methanol-air case. Sensitivity and reaction rate analyses were used to aid in recognizing the reactions to which the burning velocity is most sensitive and the principal path of methanol oxidation. Once a kinetic scheme was determined, we proceeded to establish the rich flammability limit for methanol-air flames using two different criteria: (1) composition where the burning velocity is $< 5 \text{ cm/s}$ (a qualitative rule proposed by Westbrook [1]) and (2) a kinetic criterion proposed by

Law and Egolfopoulos [2], which takes into consideration the competition between branching and termination reactions. Since both definitions yield similar results—methanol-air mixtures will not propagate beyond a composition corresponding to an equivalence ratio of 2.1, Law's criterion is chosen to calculate the critical oxygen concentration (COC) for comparison with experimental cases using Sandia's 1-D, freely-propagating premixed flame code [3]. The COC predictions from steady flame studies are much too high compared to experimental data; therefore efforts were made to model the spherical experiment directly using an ignition source code [4].

Experimental Set-up

The experiment was conducted in a 35-liter vessel. Methanol vapor is introduced into the evacuated vessel, then carbon monoxide, nitrogen or carbon dioxide, and oxygen gases were sequentially loaded. Once the mixture reached equilibrium temperature and pressure, ignition was attempted with a fuse wire (~ 1 Joule of energy), M-103 match, or chemical ignitors attached to centrally located electrodes. The explosion pressure was recorded on the Nicolet oscilloscope as well as into the data acquisition system through a high-speed card. The post ignition gases were then diluted and purged out the vessel, which underwent several evaluation cycles.

Table 1 shows nine experimental runs, of these five were compared with theoretical predictions of critical oxygen concentration. These five cases (# 3, 4, 5, 7, and 8) were performed for a ratio of CH_3OH/CO equal to 2:1 in oxygen diluted with either carbon dioxide or nitrogen at $T = 403$ K. From Table 1, cases 3 and 4 of the experiments yield critical oxygen concentrations (COC) of 10.4 ± 0.4 and 10.2 ± 0.4 for N_2 and CO_2 as diluent, respectively. The effect of heat capacity would normally increase the COC by $\sim 1\text{-}2\%$ O_2 when the diluent is CO_2 compared to N_2 . Although the observed COC for CO_2 is 10.2, this value is still within experimental accuracy range. Cases 4, 5, and 7 are identical except for pressures being 1 atm, 11.4 atm, and 21.4 atm, respectively. The interesting feature of these three cases is that the critical oxygen concentration at 11.4 atm of 5.9 is much lower than that of 8.4 at 21.4 atm. Lewis and von Elbe [5] reported that this unusual pressure effect has been noted in the past for fuel rich mixtures by Strauss and Edse [6] and Manton and Milliken [7]. These researchers observed that burning velocity decreases with increasing pressure for mixture whose burning velocity at atmospheric pressure is below approximately 50 cm/s,

and increases for mixtures whose burning velocity at atmospheric pressure is higher than this value. Strehlow [8] proposed that the change of pressure affects the dissociation equilibrium in the burned gas and also the rate of destruction of free radicals in three-body collisions. Furthermore, an increase of pressure promotes the chain-termination reaction $H + O_2 + M = HO_2 + M$ over the chain branching reaction $H + O_2 = OH + H$. Mixtures having burning velocities above approximately 50 cm/sec have high flame temperatures that are responsive to repression of dissociation by pressure increase. Therefore, as the pressure is increased, the temperature of the burned gas increases, resulting in a heightened temperature profile of the combustion wave, increased reaction rate and consequent increase of the burning velocity. Mixtures having burning velocities below approximately 50 cm/sec have low flame temperatures that are much less affected by dissociation. Such mixtures, however, are sensitive to the effect of pressure on the rates of ternary free radical reactions. Thus, an increase of pressure decreases the concentration of free radicals in the reaction zone, resulting in a decrease of burning velocity. The exact pressure range where the burning velocity would be maximized, or the critical oxygen concentration minimized, was not given in the literature or determined by the current set of experiments. How far the COC increases with further pressure increase is unclear. At some point, however, between 1 and 21.4 atm, the critical oxygen concentration reaches a minimum value and then increases.

Case 7 is the same as 8 except that the diluent is CO_2 instead of N_2 . The effect of heat capacity would normally increase the COC by $\sim 1\text{-}2\%$ O_2 when the diluent is carbon dioxide compared to nitrogen; this effect is more evident in the higher pressure range than atmospheric cases.

Formulation for the numerical problem

Chemical Kinetic Mechanism

The present kinetic scheme is derived mostly from Miller and Melius [9] with some improvements. The main modifications are the following:

1. The new rate used for the most important chain branching reaction $OH + O = H + O_2$ comes from Masten et al. [10]; this rate coefficient is consistent with Hessler's measurements at very high temperature [11] and also agrees with Miller's trajectory calculations using Varandas's potential energy surface over a very wide temperature

range. The rate expression $k_f = 2.02 \times 10^{14} T^{-0.4} \text{ cm}^3/\text{mole-sec}$ appears to represent accurately the kinetic data available from below room temperature to above 5000 K [12], where the subscript *f* indicates the forward direction of the reaction.

2. The methanol mechanism is derived principally from compilations by W. Tsang, the National Institute of Standards and Technologies [13], and the European group (CEC) [14].
3. Two different rate coefficients for $CH_3O + M = CH_2O + H + M$ were tested: (1) $k_f = 1.9 \times 10^{26} T^{-2.7} \exp(-30600/RT) \text{ cm}^3/\text{mole-sec}$ estimated by Miller [12], and (2) $k_f = 5.45 \times 10^{13} \exp(-13497/RT) \text{ cm}^3/\text{mole-sec}$ measured by Choudhury et al. [15].

The kinetic scheme consists of 123 reactions involving 28 chemical species (it does not contain any non-oxygen carrying C_2 or C_3 and higher species). Due to the length restriction, the mechanism is not listed here but can be obtained from the authors.

Governing Equations

Freely Propagating Premixed Flame

The mathematical formulation for a steady, planar, adiabatic deflagration at low Mach number has been discussed extensively in literature [3] and will not be repeated here. The mass flow rate \dot{M} is an eigenvalue and must be determined as part of the solution; therefore, in addition to the usual boundary conditions, the location of the flame is chosen to be fixed by specifying the temperature at one point. This is sufficient to allow for the solution of the flame speed eigenvalue. As an improvement over the previous formulation, thermal diffusion and multicomponent transport [16] are included, and central differencing techniques are used. This flame configuration is also employed to determine the rich flammability limit of pure methanol-air flames and CH_3OH/CO /diluent mixtures. The methods to calculate flammability limits are discussed in the Results and Discussions section of the paper.

Strained, Opposed Premixed Flame

To complete the analysis of premixed methanol-air flames, it is our judgment that it would be beneficial to establish the extinction limit for at least the stoichiometric condition, although experimental data are not available at this time. The configuration used in these calculations

is one of strained, opposed premixed flames; the detailed description can be found in Ref. [17]. The mixture composition, temperature, and the inlet velocity are specified at the nozzle exit and symmetry conditions are applied at the stagnation or symmetry plane. The nozzle separation distance for the present calculations is 7mm. In this fixed-domain approach, inlet velocity is purely axial at $x = -L$, and the radial pressure gradient eigenvalue is computed. The extinction limit is calculated with the aid of an arc length continuation method. Given a solution at point 1, the goal is to calculate the solution at point 2 efficiently. Using the normalized arc length continuation method, the relationship between the two points can be written as:

$$\Delta s = \sqrt{\left(\frac{T_{max,2} - T_{max,1}}{T_{max,1}}\right)^2 + \left(\frac{U_2 - U_1}{U_1}\right)^2}. \quad (1)$$

This procedure involves a change of variables, where the independent parameter (velocity) becomes a dependent variable, and the arc length Δs becomes the parameter. Equation (1) is then solved together with the other governing equations for a specified value of Δs (which decreases in value as the extinction limit is approached). The most important feature of the continuation procedure is its behavior near the extinction limit—a turning point in the solution (where vertical tangency occurs in the classic *S* curve). At this point, the Jacobian of the original system is singular, whereas the Jacobian of the augmented system is well behaved. Therefore, this method is a great tool in accurately predicting flame extinction limits.

Ignition Modeling

The results from steady flame studies did not yield critical oxygen concentrations that were in precise agreement with experimental data; therefore, the Sandia's ignition code [4] was used to model the experiment directly. The ignition model solves one-dimensional transport equations in Lagrangian coordinates for a spherically symmetric chamber. The details of the model development appeared in Raffel et al. [18]. To minimize the computational expense, a shorter reaction mechanism was used in the ignition simulations. Comparison of steady flame calculations using the full mechanism and the simplified one showed that the smaller mechanism predicted the same flame speed accurately. In addition, rather than computing the ignition process on the same domain as the experiments, we chose an outer radius of 4 cm. This choice is justified in light of the observation that the failure of flames to propagate occurs soon after ignition, rather than after the flame has propagated away from the initial

kernel. Furthermore, the ignition model does not consider heat loss to the surroundings, so it cannot attempt to simulate quenching effects in the experimental apparatus.

Results and Discussions

Burning Velocity

Figure 1 represents the sensitivity analysis for methanol-air premixed flames, and it reveals that as the flame becomes richer, the importance of the methoxy dissociation reaction increases. A comparison of theoretical predictions of burning velocity for methanol-air premixed flames with experimental measurements [19] can be found in Fig. 2 to exhibit good agreement, especially at lean to stoichiometric conditions. At stoichiometry, the location of the theoretical compared to measured temperature peaks exhibits a slight shift—experimental data show a temperature maximum at $\phi \sim 1.1$, whereas theoretical predictions yield a maximum at $\phi \sim 1.2$. Furthermore, the theory gives a more robust rich flame than that observed in the experiments; therefore, the theoretical burning velocity for $\phi \geq 1.3$ is slightly higher than experimental measurements. The smooth line represents results using a rate coefficient of $k_f = 1.9 \times 10^{26} T^{-2.7} \exp(-30600/RT) \text{ cm}^3/\text{mole-sec}$ for $CH_3O + M = CH_2O + H + M$, and the dashed line shows calculations using $k_f = 5.45 \times 10^{13} \exp(-13497/RT) \text{ cm}^3/\text{mole-sec}$ (Choudhury et al. [15]) for the same reaction. With this modification in the mechanism, we see an average drop of 1-3 cm/s in burning velocity yielding a significant improvement on the rich side of the flame, and although the lean to stoichiometric region shows a larger discrepancy than before, the difference is still within experimental uncertainties. Therefore, Choudhury's rate coefficient was incorporated into our mechanism to test the experimental cases conducted by Dow Chemical/Midland.

Extinction Limit

For the opposed-flow, strained premixed flame computations, a stretch parameter K is defined as the maximum axial velocity gradient $-du/dx$, as shown in Fig. 3. The velocity profile in Fig. 3 is initially that of a stagnation flow characterized by the specified negative slope. It reaches a minimum, then increases due to thermal expansion, and finally, when heat release is complete, it decreases in accordance with the stagnation flow requirement. A plot of maximum temperature as a function of the reciprocal stretch rate, $1/K$, for methanol-air

Figure 1

Figure 2

Figure 3

flames are shown in Fig. 4. A vertical tangent can be drawn where the flame is extinguished, and Fig. 4 give a value of $K_{ex} = 1780 \text{ sec}^{-1}$ and $T_{max} = 1684 \text{ K}$ for a stoichiometric methanol-air flame using the original rate for $CH_3O + M \rightleftharpoons CH_2O + H + M$ and $K_{ex} = 1670 \text{ sec}^{-1}$ and $T_{max} = 1686 \text{ K}$ using Choudhury's rate coefficient. Given the better agreement in the burning velocity comparison with experiments in the previous section, it is probable that this lower extinction limit is the correct one, although there is no evidence to support this conclusion due to lack of experimental data.

Figure 4

Flammability Limit

Although the definition of flammability limit is clear, i.e., the state at which steady propagation of the one-dimensional, planar premixed flame in the doubly-infinite domain fails to be possible [20], the theoretical determination of such limit remains problematical [21]. In this work, we compare two limits based on different criteria:

1. the critical composition which produces a burning velocity of 5 cm/s (Because the model is adiabatic, it will continue to calculate flame propagation at any equivalence ratio, although the burning velocity will be small; Westbrook [1] reported a qualitative rule that $V_u < 5 \text{ cm/s}$ corresponds to a nonflammable mixture.)
2. the critical composition where the rate of the primary chain-termination reaction equates with that of the chain-branching reaction (Law and Egolfopoulos [2]).

Employing the above criteria, we observe from Fig. 2 (dashed line) that $\phi = 2.1$ renders a burning velocity of 5 cm/s. To use Law's criterion, a sensitivity analysis was conducted for a rich condition ($\phi = 2.0$) to establish the appropriate chain-branching and chain-termination reactions. Figure 1 shows that these reactions are $H + O_2 \rightarrow OH + O$ and $HO_2 + H \rightarrow O_2 + H_2$, respectively. Once the dominant branching and termination paths are identified, it is found that their respective rate profiles approach each other at the flammability limit. In order to establish a quantitative critical composition, a parameter α (termed the flammability exponent) was proposed by Law and Egolfopoulos [2] to be $\alpha = \partial(\ln\omega_T)/\partial(\ln\omega_B)$, where $\omega \equiv \text{net rate}$, and T and B denote termination and branching, respectively. The critical composition where $\alpha = 1$ represents the flammability limit, and from our calculations, $\alpha = 1$ at $\phi = 2.2$ for pure methanol-air flames. The Dow case #5 is chosen to illustrate these phenomena. Fig. 5 presents the temperature at the maximum rate of the main termination

Figure 5

and branching reactions as a function of oxygen mole fraction, and it can be seen that the two temperature profiles merge at the critical limit. Figure 6 contains the flammability exponent as a function of oxygen mole fraction; the composition where $\alpha = 1$ coincides with that in Fig. 5 where the two temperature profiles meet. Figure 6

Since both definitions yield similar results for rich methanol-air flammability limit, Law's criterion was employed to calculate the critical oxygen concentrations for comparison with experiments. Sensitivity analyses were conducted for all cases to be compared with experimental data to reveal that the main chain-branching and termination reactions are similar to those of rich methanol-air flames, and they are $H + O_2 \rightarrow OH + O$ and $HO_2 + H \rightarrow O_2 + H_2$, respectively. Cases 3 and 4 yield critical oxygen concentration predictions of 14.7% and 15.6% for N_2 and CO_2 as diluent, respectively. The effect of heat capacity was not evident experimentally; however, this effect was captured in the model where the critical oxygen concentration is higher (about 1%) when the diluent is CO_2 instead N_2 . Cases 4, 5, and 7 are identical except for pressures being 1 atm, 11.4 atm, and 21.4 atm, and the calculations reveal that COC are 15.6%, 14.4%, and 15.2%, respectively. The unusual pressure effect where the intermediate pressure displays a lower COC than the high pressure is clearly observed both in experiments and in the model. Case 7 is the same as 8 except that the diluent is CO_2 instead of N_2 ; case 8 yields a critical oxygen concentration of 13.4%. The effect of heat capacity would normally increase the COC by $\sim 1\text{-}2\%$ O_2 when the diluent is carbon dioxide over that when it is nitrogen; in our model, this effect is more evident in the higher pressure case (difference of 1.8%) than in the atmospheric case (0.9%).

Ignition Modeling

Since there seems to be a large quantitative difference between our theoretical predictions and the experimental data, we have attempted to reconcile the differences by simulating the experiments as closely as possible. We do this by utilizing the ignition code described above. Figure 7 shows the computed pressure rise for a series of ignition computations in a 2 to 1 methanol/carbon monoxide mixture with various quantities of oxygen and diluted with nitrogen. The initial conditions of the mixture were 403 K and 1 atm (case 3). To approximate the experimental spark ignition, the source added 1 J of energy in a radius of 0.8 cm at a constant rate during the first 0.1 sec of the simulation. The solid curve represents the equilibrium pressure for adiabatic combustion at constant volume. The circles Figure 7

show the results of the ignition modeling. The simulations predict a flammability limit of roughly 13 percent oxygen (which is relatively close to the steady flame result of 14.7%), while the experimental limit occurs around 10.4 percent. Thus, there seem to be some legitimate differences between both models and experiments; these discrepancies warrant further research.

Concluding Remarks

In the present investigation, we have explored the possibility of applying existing flame modeling capability developed at Sandia National Laboratories to model industrial processes. This joint project with Dow Chemical Company/Midland involves efforts in modeling and predicting flammability limits for systems burning methanol/carbon monoxide in oxygen with either nitrogen or carbon dioxide as diluent and comparing theoretical results with experimental data. The theoretical critical oxygen concentration predictions agree qualitatively with experiments, although there are still quantitative differences; thus an attempt was made to model the spherical experiment. Case 3 (described above) was compared with experimental results to yield better agreement than that produced by the freely-propagating model, although quantitative discrepancies still exist. The rich flammability limit and extinction limit for the stoichiometric case were calculated for methanol-air flames to render a flammability limit at $\phi = 2.1$ and an extinction limit of $K_{ex} = 1670 \text{ sec}^{-1}$ for $\phi = 1.0$ for a nozzle separation distance of 7 mm. Experimental data are needed for comparison with these predictions.

Acknowledgements

This research is supported by the Department of Energy through the Office of Basic Energy Sciences, Division of Chemical Sciences. MNBP also would like to thank Ms. Fran Rupley for her assistance with the computer codes.

DISCLAIMER

This report was prepared as an account of work sponsored by an agency of the United States Government. Neither the United States Government nor any agency thereof, nor any of their employees, makes any warranty, express or implied, or assumes any legal liability or responsibility for the accuracy, completeness, or usefulness of any information, apparatus, product, or process disclosed, or represents that its use would not infringe privately owned rights. Reference herein to any specific commercial product, process, or service by trade name, trademark, manufacturer, or otherwise does not necessarily constitute or imply its endorsement, recommendation, or favoring by the United States Government or any agency thereof. The views and opinions of authors expressed herein do not necessarily state or reflect those of the United States Government or any agency thereof.

References

1. Westbrook, C. K., *Nineteenth Symposium (International) on Combustion*, p. 127 (1982).
2. Law, C. K. and Egolfopoulos, F. N., *Twenty-third Symposium (International) on Combustion*, p. 413 (1990).
3. Smooke, M. D., Miller, J. A., and Kee, R. J., *Combust. Sci. Tech.* 34:79 (1983).
4. Lutz, A. E., personal communication.
5. Lewis, B. and von Elbe, G., *Combustion, Flames, and Explosions of Gases*, Third edition, Academic Press, Orlando, 1987, p. 408.
6. Strauss, W. A. and Edse, R., WADC Technical Report 56-49, *Seventh Symposium on Combustion*, Butterworths, London, 1959, p. 377.
7. Manton, J. and Milliken, B. B.; cf. Lewis, B., *Selected Combustion Problems* (AGARD), Butterworths, London, 1954, p. 117.
8. Strehlow, R. A., *Combustion Fundamentals*, McGraw-Hill, New York, 1984, p. 283.
9. Miller, J. A. and Melius, C. F., *Combust. Flame* 91:21 (1992).
10. Masten, D. A., Hanson, R. K., and Bowman, C. T., *J. Phys. Chem.*, p. 7119 (1990).
11. Du, H. and Hessler, J. P., *J. Chem. Phys.*, 96:1077 (1992).
12. Miller, J.A., personal communication.
13. Tsang, W., *J. Phys. Chem. Ref. Data*, p. 471 (1987).
14. Grotheer, H., Kelm, S., Driver, H. S. T., Hutcheon, R. J., Lockett, R. D., and Robertson, G. N., *Ber. Bunsenges. Phys. Chem.*, p. 1360, (1992).
15. Choudhury, T. K., He, Y., Sanders, W. A., and Lin, M. C., *J. Phys. Chem.*, p. 2394 (1990).
16. Kee, R. J., Dixon-Lewis, G., Warnatz, J., Coltrin, M. E., and Miller, J. A., Sandia Report, SAND86-8246 (1986), reprinted July 1992.

17. Kee, R. J., Miller, J. A., Evans, G. H., and Dixon-Lewis, G., *Twenty-Second Symposium (International) on Combustion*, p. 1479 (1988).
18. Raffel, B., Warnatz, J., Wolff, H., Wolfrum, J., and Kee, R.J., *Dynamics of Reactive Systems Part II: Modeling and Heterogeneous Combustion* (Bowen, J. R., Leyer, J.C., and Soloukhin, R. I., Eds.), American Institute of Aeronautics and Astronautics, Inc., New York, New York, 1986, p. 335.
19. Egolfopoulos, F. N., Xu, D. X., and Law, C.K., *Combust. Sci. Tech.* 83:33 (1989).
20. Spalding, D. B. *Proc. R. Soc. London A* 240, p. 83 (1957).
21. Lakshmisha, K. N., Paul, P. J., Rajan, N. K. S., Goyal, G., and Mukunda, H.S., *Twenty-Second Symposium (International) on Combustion*, p. 1573 (1988).

List of Tables and Figures

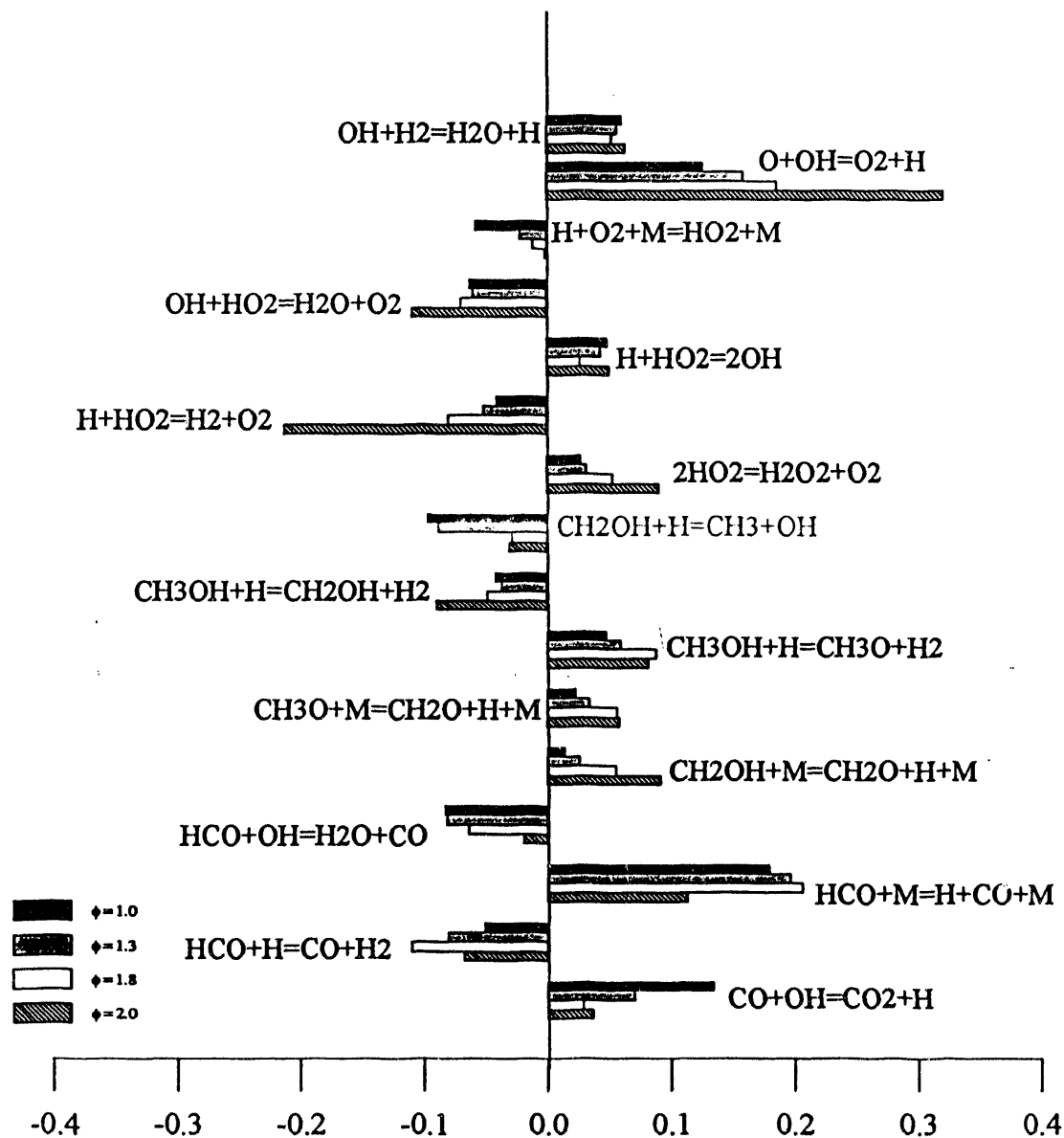
Table 1. Experimental results for critical oxygen concentration.

1. Figure 1. Sensitivity for the mass burning rate for freely propagating premixed flame.
2. Figure 2. Burning velocity as a function of equivalence ratio ϕ for freely propagating premixed flame.
3. Figure 3. Axial velocity profile of a strained premixed flame.
4. Figure 4. Maximum flame temperature as a function of the reciprocal stretch rate, $1/K_{ex}$ for stoichiometric methane-air premixed flame.
5. Figure 5. Temperature profile at maximum branching and termination rate as a function of mole fraction of oxygen.
6. Figure 6. Flammability exponent α as a function of mole fraction of oxygen.
7. Figure 7. Pressure ratio as a function of oxygen concentration for spherical model.

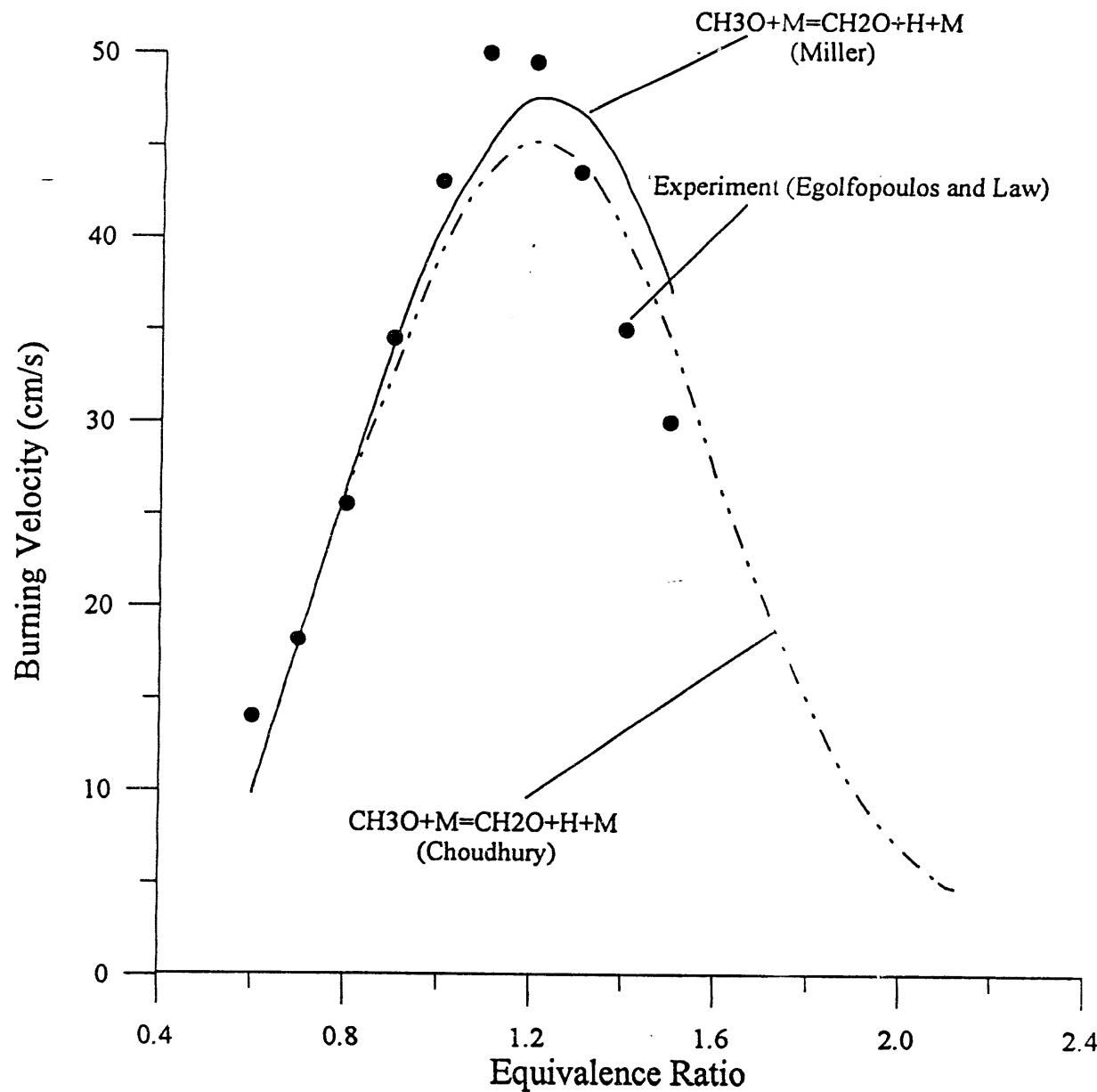
Table 1: Experimental Results

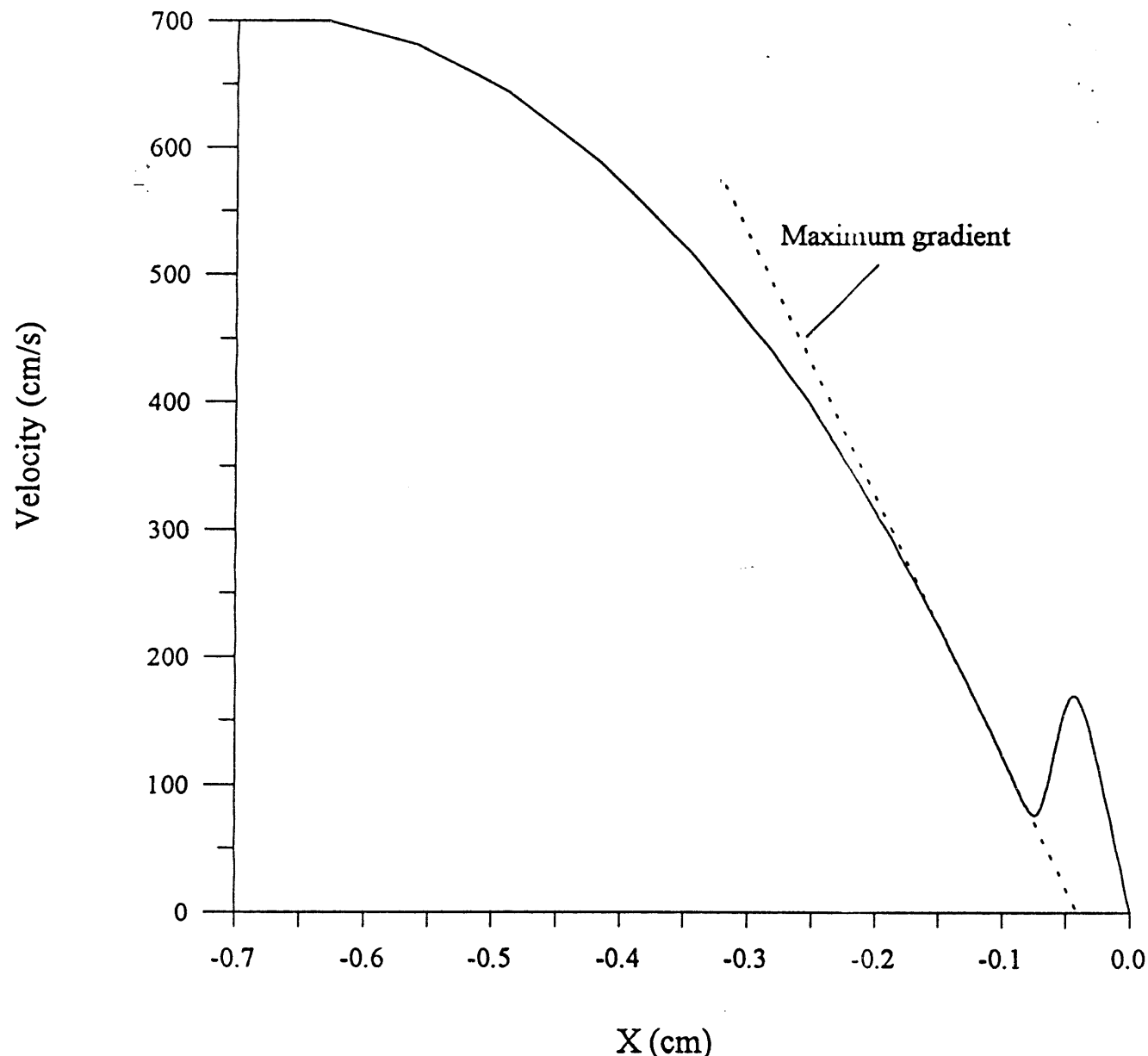
Case	P (atm)	T (K)	<i>CH₃OH</i>	<i>CO</i>	Diluent	COC
1	1	333	0	30	<i>N</i> ₂	6.0 ± 0.2
1	1	333	30	0	<i>N</i> ₂	12.0 ± 0.5
3	1	403	20	10	<i>N</i> ₂	10.4 ± 0.4
4	1	403	20	10	<i>CO</i> ₂	10.2 ± 0.4
5	11.4	403	20	10	<i>CO</i> ₂	5.9 ± 0.2
6	21.4	403	10	20	<i>CO</i> ₂	6.9 ± 0.3
7	21.4	403	20	10	<i>CO</i> ₂	8.4 ± 0.3
8	21.4	403	20	10	<i>N</i> ₂	6.6 ± 0.2
9	21.4	403	30	15	<i>CO</i> ₂	10.9 ± 0.4

Methanol-Air Premixed Flames

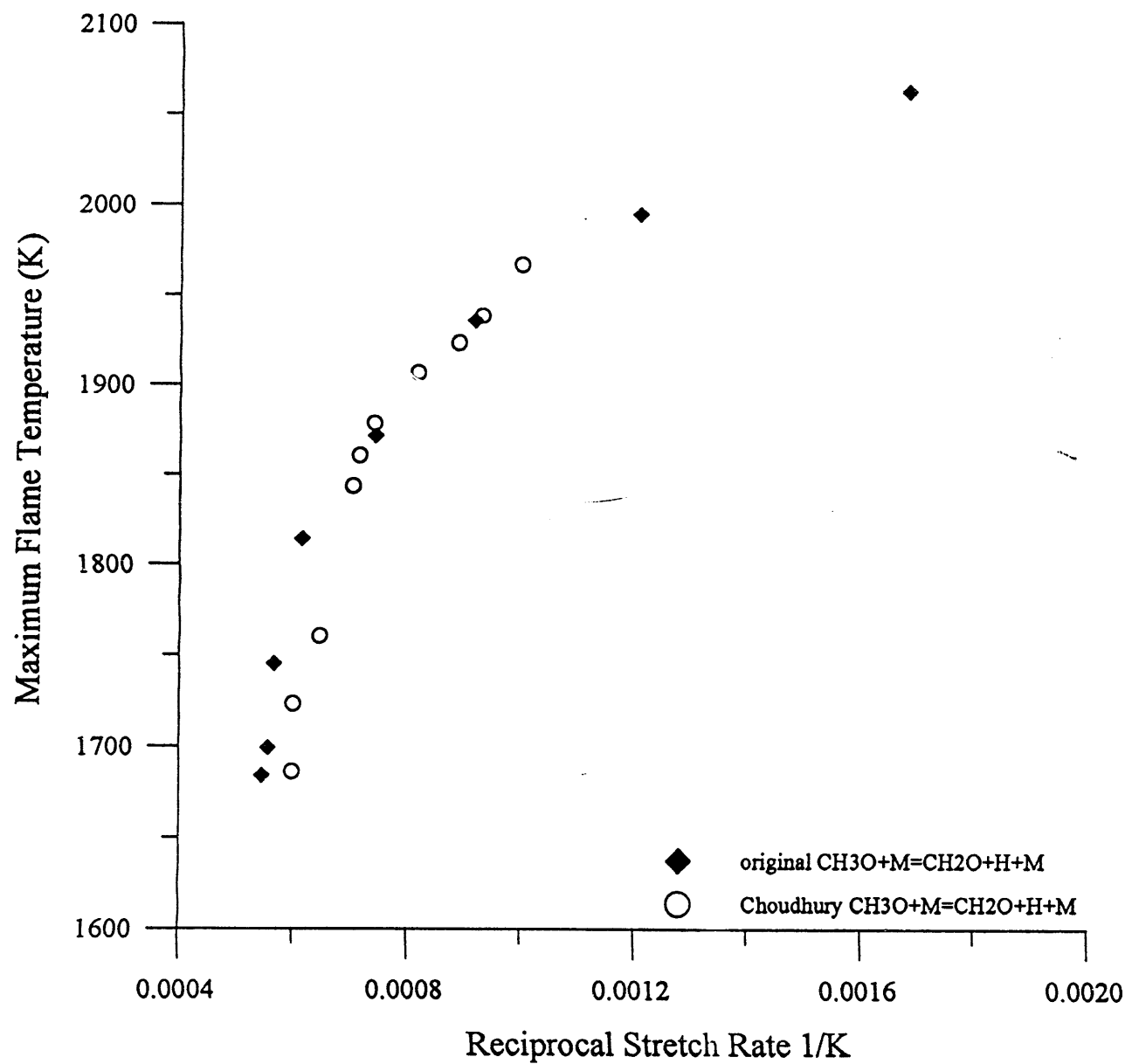


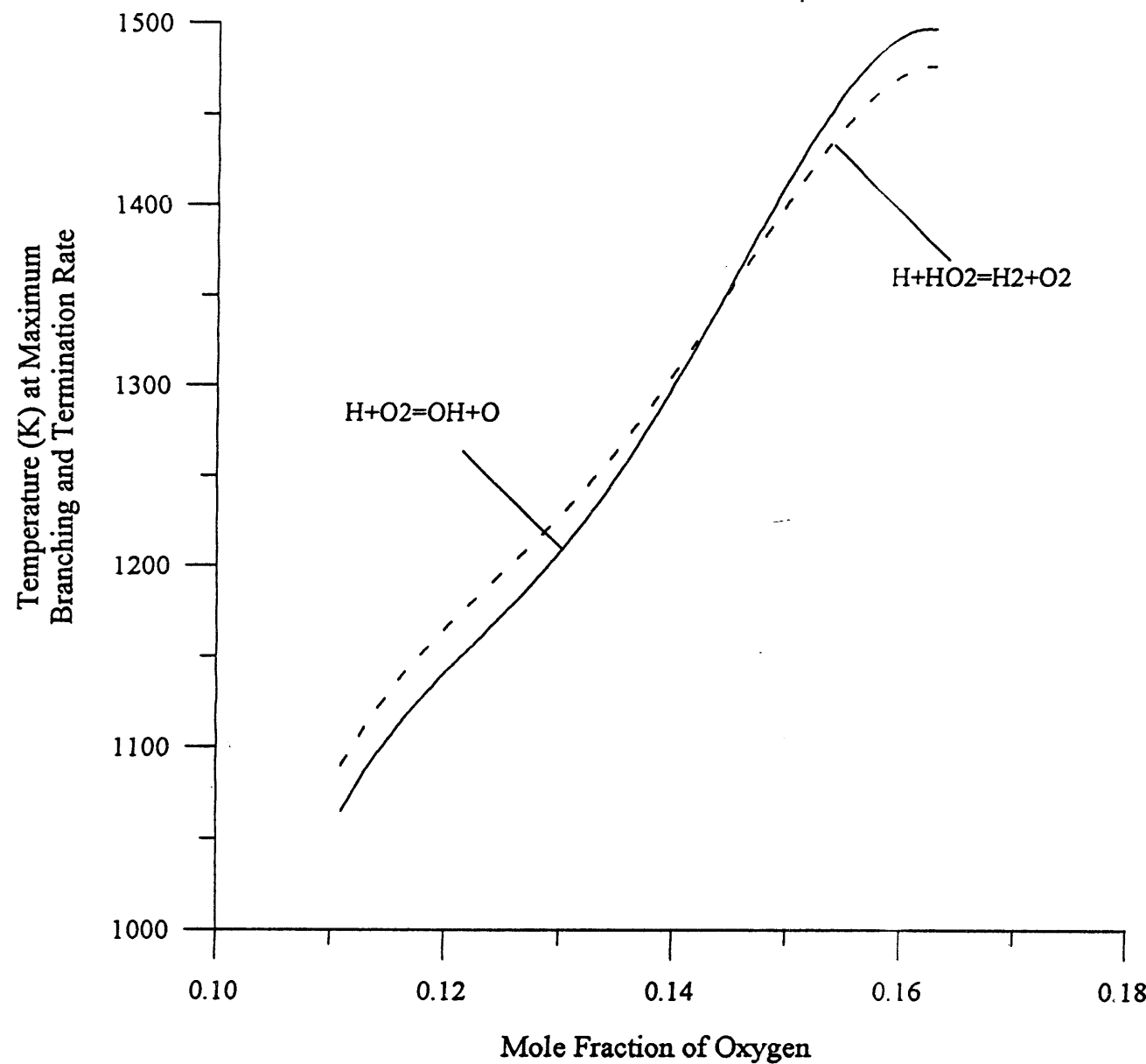
Methanol-Air Premixed Flame

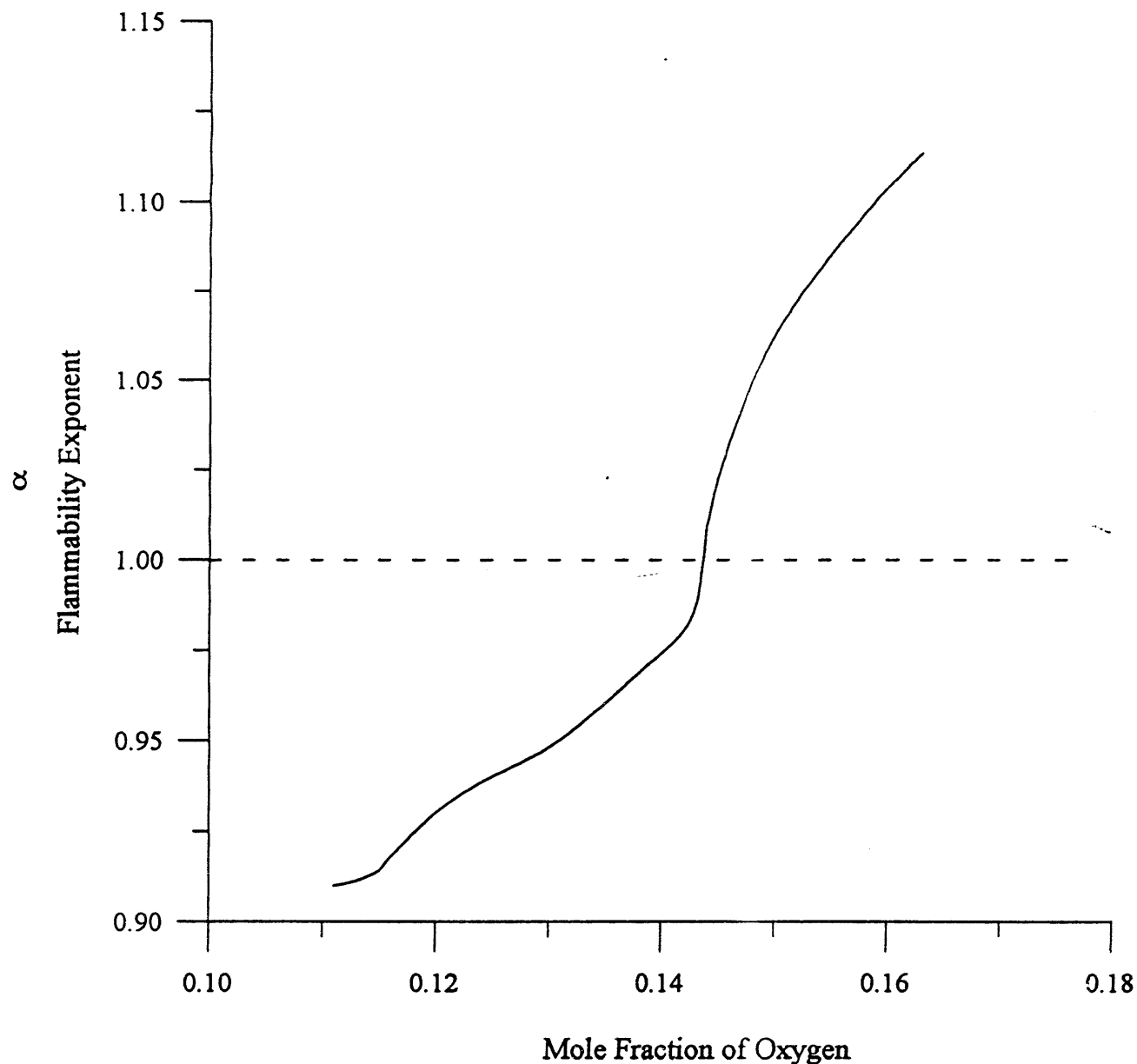


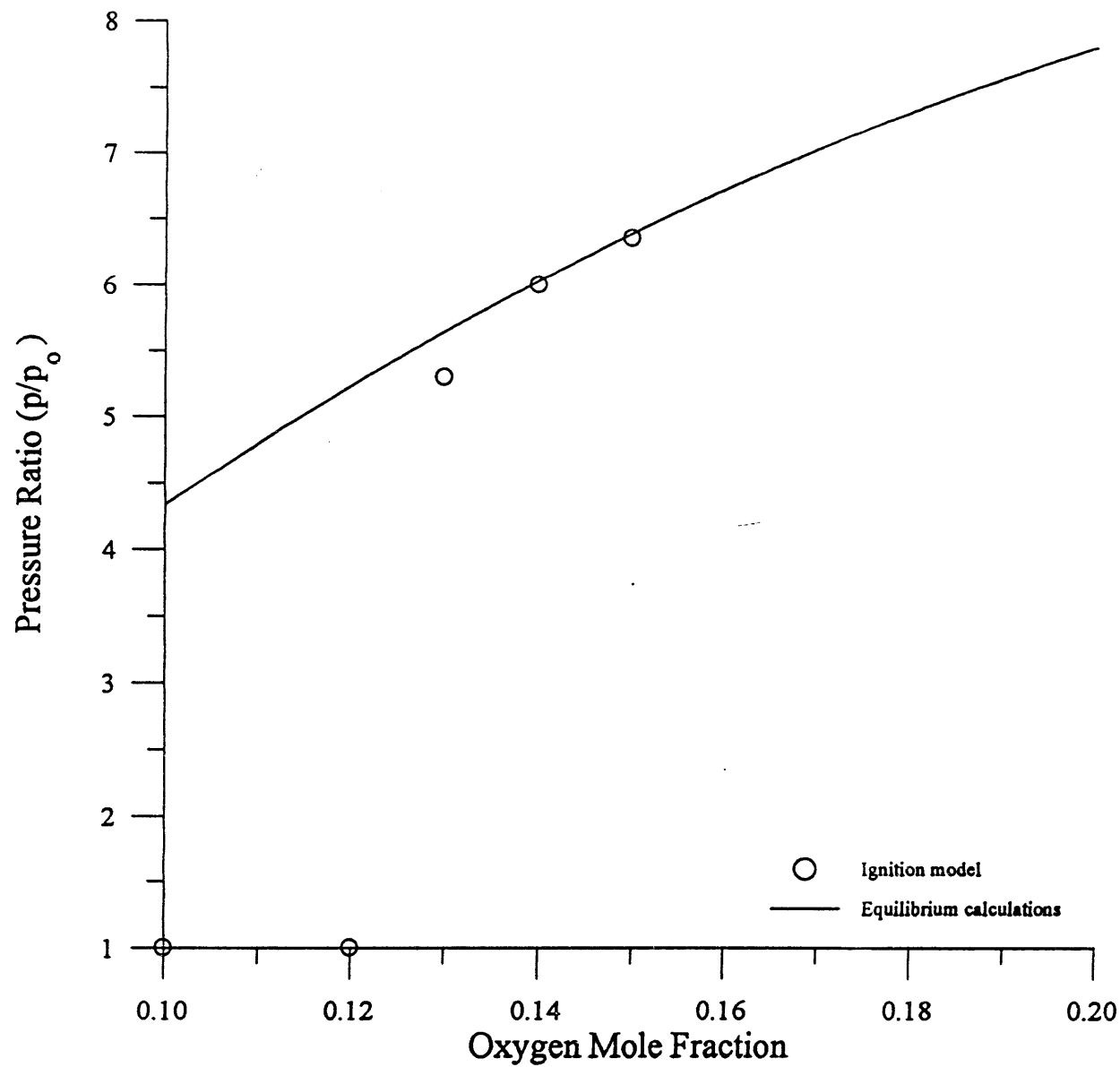


Opposed-Flow, Strained Methanol
Premixed Flame









100
500
1000
5000

DATE
MEDLINE
1990/10/16
MEDLINE

